



This is a repository copy of *Interplay among electrostatic, dispersion and steric interactions: Spectroscopy and quantum chemical calculations of π -hydrogen bonded complexes*.

White Rose Research Online URL for this paper:
<http://eprints.whiterose.ac.uk/111278/>

Version: Accepted Version

Article:

Kumar, S., Singh, S.K., Vaishnav, J.K. et al. (2 more authors) (2017) Interplay among electrostatic, dispersion and steric interactions: Spectroscopy and quantum chemical calculations of π -hydrogen bonded complexes. *ChemPhysChem*, 18 (7). pp. 828-838. ISSN 1439-71439

<https://doi.org/10.1002/cphc.201601405>

Reuse

Items deposited in White Rose Research Online are protected by copyright, with all rights reserved unless indicated otherwise. They may be downloaded and/or printed for private study, or other acts as permitted by national copyright laws. The publisher or other rights holders may allow further reproduction and re-use of the full text version. This is indicated by the licence information on the White Rose Research Online record for the item.

Takedown

If you consider content in White Rose Research Online to be in breach of UK law, please notify us by emailing eprints@whiterose.ac.uk including the URL of the record and the reason for the withdrawal request.



eprints@whiterose.ac.uk
<https://eprints.whiterose.ac.uk/>

Interplay among electrostatic, dispersion and steric interactions: Spectroscopy and quantum chemical calculations of π -hydrogen bonded complexes

Sumit Kumar,^{[a] #} Santosh K. Singh,^{[a] \$} Jamuna K. Vaishnav,^{[a] †} J. Grant Hill^[b] and Alope Das^{*[a]}

Abstract: π -hydrogen bonding interactions are ubiquitous in both materials and biology. Despite their relatively weak nature great progress has been made in their investigation by experimental and theoretical methods, but this becomes significantly more complicated when secondary intermolecular interactions are present. In this study the effect of successive methyl substitution on the supramolecular structure and interaction energy of indole...methylated benzene (ind...*n*-mb, $n = 1-6$) complexes is probed through a combination of supersonic jet experiment and benchmark quality quantum chemical calculations. It is demonstrated that additional secondary interactions introduce a subtle interplay among electrostatic and dispersion forces, as well as steric repulsion, which fine-tunes the overall structural motif. Resonant Two-Photon Ionization (R2PI) and IR-UV double resonance spectroscopy techniques were used to probe jet-cooled ind...*n*-mb ($n = 2, 3, 6$) complexes, with red-shifting of the N-H IR stretching frequency showing that increasing the degree of methyl substitution increases the strength of the primary N-H... π interaction. *Ab initio* harmonic frequency and binding energy calculations confirm this trend for all six complexes. Electronic spectra of the three dimers are broad and structureless, with quantum chemical calculations revealing that this is likely due to multiple tilted conformations of each dimer possessing similar stabilization energies.

Introduction

π -hydrogen bonding interaction plays a pivotal role in the structures of biomolecules and materials as well as biomolecular recognition processes.^[1-11] This interaction generally occurs between an X-H donor (X= N, O, S, C etc.) and a π -electron cloud of an aromatic moiety,^[9] and has been explored in great detail over the past few decades through various methods like X-ray crystallographic studies, FT-IR, isolated gas phase studies and quantum chemical calculations.^[9-54] It has been noticed that local arrangements and orientations of the X-H... π hydrogen bonding interactions in biomolecules are quite intriguing.^[8-9, 12-13, 35] Steiner et al. have performed Protein Data Bank (PDB) analysis of high resolution crystal structures of 593 proteins and found that every 11th aromatic residue in the side chain of proteins is engaged by this interaction.^[11] Malone et al. have investigated the preferred geometries and selective orientations of X-H... π (phenyl) interactions based on Cambridge Structural Database (CSD) mining along with semi-empirical calculations and reported that more than 50% of N-H... π interactions have a direct interaction of N-H with carbon atoms of the phenyl ring present in proteins.^[12] Worth and Wade, in addition to Mitchell and co-workers, have also performed analysis of crystallographic databases of proteins and found that N-H... π interaction, in comparison to other types of π -hydrogen bonding interactions like C-H... π , O-H... π etc., has high propensity to occur in proteins. Hence, detailed study of the N-H... π interaction at the quantitative level is important.^[13, 32]

Given the importance and delicate nature of this weak π -hydrogen bonding interaction, gas phase experiments and theoretical studies are well-suited to explore it at the molecular level.^[14-26, 38-52] Indeed, a combination of both theory and experiment is often required for a quantitative understanding of the strength, binding motif and underlying nature of many weak intermolecular

interactions.^[55-57] This is challenging for several reasons, on the experimental side it is generally difficult to find out the presence of multiple conformations of the complexes with similar binding energies due to low interconversion barrier or their broad electronic spectra and overlapping IR frequencies even in isolated gas phase. From a theoretical point of view, π -hydrogen interactions require a method that provides a balanced description of both electrostatic and dispersion forces; overemphasis of one component is likely to lead to an artificial favoring of incorrect conformations. Basis set superposition error (BSSE) can also be problematic for both interaction energies and structures unless a correction such as the counterpoise (CP) method of Boys and Bernardi is applied.^[58] Recent developments in fundamental theoretical chemistry provide some effective solutions to these stumbling-blocks. Explicitly correlated (F12) variants of the coupled cluster with single, double and perturbative triple excitations [CCSD(T)] method provide a route to benchmark quality interaction energies; near complete basis set (CBS) limit data becomes achievable with relatively small orbital basis sets.^[59-61] The effect of BSSE can also be

[a] Dr. S. Kumar, S. K. Singh, J. K. Vaishnav, Dr. A. Das
Department of Chemistry
Indian Institute of Science Education and Research (IISER)
Dr. Homi Bhabha Road, Pashan, Pune-411008, Maharashtra, India
E-mail: a.das@iiserpune.ac.in

[b] Dr. J. G. Hill
Department of Chemistry
University of Sheffield
Sheffield S3 7HF, UK

Present address: Department of Dynamics at Surfaces, Max Planck
Institute of Biophysical Chemistry, Am Faßberg 11, 37077
Göttingen, Germany

† Present address: Indian Institute of Technology (IIT) Indore,
Khandwa Rd, Simrol, Madhya Pradesh-452020, India

\$ Both the author's have equal contribution

Supporting information for this article is given via a link at the end of
the document.

ameliorated through local correlation methods, such as local Møller-Plesset second order perturbation theory (LMP2), that are free from BSSE in electron correlation treatment by construction.^[62] Spin-component-scaled (SCS) local correlation methods hold the promise of being accurate and computationally affordable, while avoiding the need for counterpoise correction during geometry optimization.^[63-64] The SCSN re-parameterization of SCS specifically targets weak and stacking interactions and was developed to ensure a more balanced description of hydrogen bonding and dispersion interactions than the original SCS method.^[64] This SCSN method has previously been used to successfully investigate intermolecular interactions such as those in nucleic acid base-pair steps, and between aromatic intercalators and nucleic acids.^[65-66]

The complementary nature of quantum chemical calculations and exquisite gas phase experiment for probing intermolecular interactions can be illustrated with the extensively investigated example of the benzene dimer.^[24-31, 36-37, 67-72] Only the tilted T-shaped structure (C-H $\cdots\pi$ bound) has been observed in the gas phase experiment, although both the T-shaped and the parallel displaced (PD) structures are almost isoenergetic at the CCSD(T)/CBS level of calculation.^[24-25, 36-37] Similarly the benzene \cdots NH₃ complex has been studied as a prototype for the N-H $\cdots\pi$ interaction by Rodham *et al.* using microwave spectroscopy.^[34] However, the orientation of an N-H $\cdots\pi$ interaction is not so straightforward when the interaction is between two aromatic moieties, analogous to that for the C-H $\cdots\pi$ interaction in the benzene dimer.

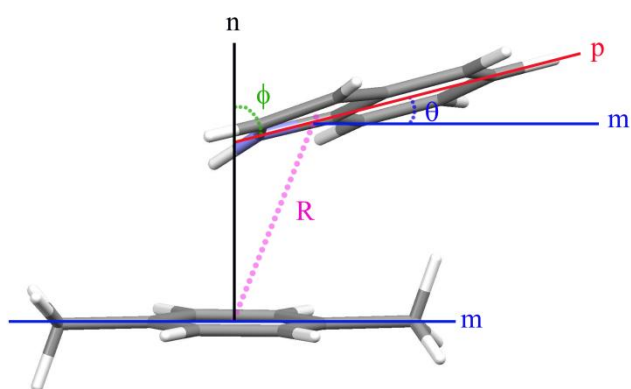


Figure 1: Schematic representation of the intermolecular geometrical parameters of indole...methylated benzene. R represents the distance between the ring centers (not mass weighted), θ represents the angle between the molecular plane of methylated benzene (m) and plane of the indole (p), ϕ represents the angle between the plane of the indole (p) and normal (n) to the plane of the methylated benzene.

Recently, Biswal *et al.* have reported that the structure of the observed conformer of the indole...benzene dimer in the gas phase experiment is a tilted T-shaped with an N-H $\cdots\pi$ hydrogen bond as the primary form of interaction.^[23] It is important to mention here that the tilt in the plane of the H-bond donor with respect to the plane of the H-bond acceptor can be defined either by an angle ϕ or θ (see Figure 1). ϕ is the angle between the plane of the H-bond donor (p) and the normal (n) to the plane of the H-bond acceptor while θ is the angle between the plane of the H-bond acceptor (m) and the plane of the H-bond donor (p). However, the angle θ has been used to define the tilt angle of the dimeric complexes discussed in this article. The tilt angle (θ) reported for the indole...benzene complex at the CP-B97-D/TZVPP level of calculation is 53.8°.^[23] A T-shaped structure with a similar tilt angle ($\theta = 55^\circ$) has been observed experimentally in the case of pyrrole dimer.^{[15], [73]} Further, the tilt angles θ in the N-H $\cdots\pi$ bound structures of 2-pyridone...benzene and pyrrole...benzene dimers are reported to be 78° and 77°, respectively.^[20-21] Das and co-workers observed N-H $\cdots\pi$ hydrogen bonded structures of indole...furan and indole...thiophene dimers with tilt angles θ of 75° and 55°, respectively.^[16-17] It should be noted that the tilt angles reported in the π -hydrogen bonded structures of 2-pyridone...benzene, pyrrole...benzene, indole...furan and indole...thiophene complexes in the literature are defined by the angle ϕ .

It is noteworthy that the gas phase experiments combined with theoretical studies show the tilted T-shaped N-H $\cdots\pi$ bound structures of aromatic dimers to be more stable than the idealized T-shaped and PD structures, while the tilt angle of the T-shaped structures varies depending upon the molecular systems chosen for the study.^[15, 20-21, 23] Thus, it is important to understand the factors which influence the tilt angle of these dimeric complexes. Detailed knowledge of these features governing the subtle change in the orientation of two monomeric units will help to tune the overall structural motifs of supramolecular assembly. The tilt in the X-H $\cdots\pi$ bound idealized T-shaped structure consisting of two aromatic moieties occurs due to additional stability originated from π - π stacking and C-H $\cdots\pi$ interactions.

The strength of the X-H $\cdots\pi$ interaction generally varies with the electron density on the π -ring in addition to the polarity of the X-H group. Methylation of the aromatic ring acting as a π -hydrogen bond acceptor can be an effective way to tune this interaction. However, methyl substitution of the aromatic ring will simultaneously affect the electrostatic, dispersion and steric components of the interaction energy in the complex. Consequently, a subtle balance of these interactions will govern the overall structural motif of the π -hydrogen bonded complexes. Surprisingly, systematic studies of the effect of methyl substitution on the π -hydrogen bonding are sparse in the literature.^[15, 22, 53, 74] In a different context, Boxer and co-workers have determined the contribution of electrostatics in π -hydrogen bonding interaction by studying vibrational stark spectroscopy of complexes of indole/phenol/thiophenol with a series of methyl substituted benzenes.^[22, 53] Recently, Das and co-workers have demonstrated how the variation of the heteroatoms in the π -hydrogen bond acceptor ring affects the strength of the interaction.^[16-17] In other work, Dauster *et al.* have studied FTIR-Jet spectroscopy of complexes of pyrrole with methyl substituted pyrroles and observed an increase in the red-shift in the N-H stretching

frequency with increasing methyl substitution in the hydrogen bond acceptor.^[15] It has been observed from IR cavity ring down spectroscopy combined with *ab initio* calculations that the interplanar angle of 2,5-dimethylpyrrole dimer is much larger than that of the pyrrole dimer.^[74]

In this work, the structures of indole...methylated benzene (ind...*n*-mb, *n*=1-6) dimers are investigated using one-color and two-color resonant two-photon ionization spectroscopy (1C- and 2C-R2PI), IR-UV double resonance spectroscopy and quantum chemical calculations. It has been observed that the geometries of these complexes, which are generally tilted T-shaped, are stabilized due to the simultaneous presence of N-H... π hydrogen bonding, π - π stacking and C-H... π interactions. The most important finding of the present investigation is observation of a subtle change in the tilt angle of the structures of the indole...methylated benzenes due to stepwise methylation of the benzene ring (π -hydrogen bond acceptor).

Results and Discussion

A. Electronic Spectra

1C-R2PI spectra measured in the mass channels of indole (ind), indole...1,4-dimethylbenzene (ind...2-mb), indole...1,3,5-trimethylbenzene (ind...3-mb) and indole...hexamethylbenzene (ind...6-mb) dimeric complexes are shown in Figures 2a-d, respectively. Figures S1, S2 and S3 in the supporting information show the TOF mass spectra of the complexes of indole in the presence of 2-mb, 3-mb and 6-mb, respectively. Figure 2a shows the origin band for the $S_1 \leftarrow S_0$ transition of indole monomer at 35240 cm^{-1} and this spectrum nicely corroborates those previously reported.^[75] Unlike the electronic spectrum of the indole monomer, the electronic spectra of all the complexes of indole studied here, i.e., ind...2-mb, ind...3-mb, and ind...6mb, show very broad and structureless features. On the other hand, the electronic spectrum of the indole...benzene complex reported in the literature exhibits only sharp features.^[23] Similar broad electronic spectra for indole...methyl benzene (ind...1-mb) and ind...2-mb complexes were reported by Hager *et al.* using laser induced fluorescence spectroscopy.^[76] They found that the broadening in the electronic spectra of these complexes did not change appreciably even at very low concentrations of 1mb and 2mb. However, the authors noted that the broad background obtained in the electronic spectrum of the indole...benzene complex mostly disappeared by lowering the concentration of benzene. Thus, they interpreted the broadening in the electronic spectra of the ind...1-mb and ind...2-mb complexes in terms of mostly the presence of many unresolved low frequency intermolecular vibrations of multiple conformers and to smaller extent the presence of higher order complexes. Observation of structureless broad electronic spectra of jet-cooled halobenzene clusters and mixed halobenzene...benzene clusters due to the presence of multiple isomers and their low frequency intermolecular modes have been reported in great detail in the literature.^[77-79]

In this work, the electronic spectra of all the three complexes are also measured at very low concentrations of 2-mb (0.023%), 3-mb (0.11%) and 6-mb (0.008%). Therefore, the contribution of the fragmentation of the higher order clusters into the dimer mass channels to the broadening in the electronic spectra shown in Figures 2b-d is minimal. Rather this broadening most likely arises due to overlapping transitions of multiple isomers and their low frequency intermolecular vibrational modes. Detailed quantum chemical calculations on multiple conformations of these complexes are described in the theoretical section.

To avoid unwanted fragmentation of the higher order clusters into the dimer mass channels, we have also measured 2C-R2PI spectra of the ind...3-mb and ind...6-mb complexes in the dimer mass channel by fixing the ionization laser at longer wavelength (347 nm). Available excess energy to the ions of these complexes with respect to the ionization potential (IP) of indole in the 2C-R2PI process is 1174 cm^{-1} while the same in the 1C-R2PI process is 7596 cm^{-1} . The 2C-R2PI spectra of the ind...3-mb and ind...6-mb complexes are provided in Figure S4 in the supporting information. The 1C-R2PI spectra of these two

complexes are also provided in the same Figure for comparative purposes. It is interesting to note that similar broadening has been observed in the 1C-R2PI and 2C-R2PI spectra of these complexes. A close inspection of Figures S4(c) and S4(d) indicates that the high energy tail and a small hump observed in the 1C-R2PI spectrum of ind...6-mb (Figure 2d) disappear in the 2C-R2PI spectrum. Thus, there is a small contribution from the fragmentation of the higher order clusters into the dimer mass channel to the broadening of the 1C-R2PI spectrum of ind...6-mb.

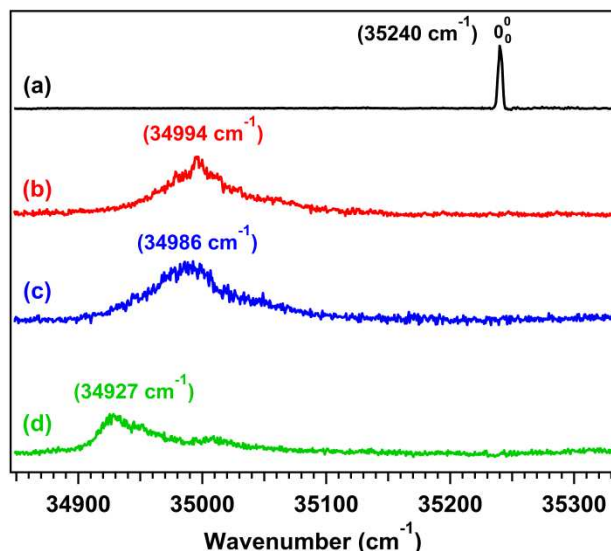


Figure 2: 1C-R2PI spectra measured in the (a) indole monomer, (b) indole-2-methylbenzene (ind-2-mb), (c) indole-1,3,5-trimethylbenzene (ind-3-mb) and (d) indole-hexamethylbenzene (ind-6-mb) dimer mass channels.

Interestingly, the TOF mass spectrum (see Figure S3 in the supporting Information) recorded by fixing the laser wavelength at the band maxima (34927 cm^{-1}) of the indole-6-mb dimer reveals the formation of an indole-6-mb-H₂O complex which might fragment to the indole-6-mb complex. In fact, the R2PI spectrum measured in the indole-6-mb-H₂O trimer mass channel (see Figure S5 in the supporting information) resembles the small hump observed in the R2PI spectrum of the indole-6-mb dimer. Similar fragmentation of a trimer into a dimer mass channel has also been reported in our previous studies on indole-furan and indole-pyridine complexes.^[16, 18] It is worth mentioning here that the TOF mass spectra (Figures S1 and S2 in the supporting information) of indole in the presence of 2-mb and 3-mb do not show any higher order clusters of indole-2-mb or indole-3-mb complexes.

The electronic spectra presented in Figures 2b-d show that the band maxima of indole-2-mb, indole-3-mb and indole-6-mb dimers are red shifted by 246, 254 and 313 cm^{-1} , respectively, from the origin band of the indole monomer. As the electronic bands of these complexes are extremely broad, it is not possible to assign the origin band of these complexes. However it is clear that the band maxima of the complexes move towards red as the methyl substitution in the benzene ring increases.

B. IR spectra

To determine the structures of the indole-2-mb, indole-3-mb and indole-6-mb dimers observed in the experiment, IR spectra have been measured in the NH stretching frequency region using RIDIR spectroscopy. The IR spectrum presented in Figure 3a shows free NH stretching frequency of the indole monomer at 3526 cm^{-1} by probing its origin transition. A similar value for the free NH stretching frequency of the indole monomer has been reported in the literature.^[80] Figures 3b-d show IR spectra by probing the band maxima of the indole-2-mb, indole-3-mb and indole-6-mb dimers. The IR bands for the N-H stretching vibration in the dimers are red-shifted from that in the bare indole by 65, 73 and 97 cm^{-1} , respectively. It is instructive to note that indole-benzene dimer studied in the gas phase is reported to be bound by N-H $\cdots\pi$ hydrogen bonding interaction with a red-shift of 47 cm^{-1} in the N-H stretching frequency.^[23] Thus the IR data obtained here demonstrate that the dimeric complexes of indole and methylated benzenes could also be stabilized by N-H $\cdots\pi$ hydrogen bonding interaction. However, the red-shift in the N-H stretching frequency increases systematically with the increase of the methyl substitution in the benzene ring. In a

different context, in order to quantify the electrostatic component in the X-H $\cdots\pi$ hydrogen bonds, Boxer and co-workers measured solution phase FTIR spectra of indole in mixtures of substituted benzenes and CCl₄.^[22] They observed red-shift of 59, 66, and 88 cm^{-1} in the N-H stretching frequency of indole in the presence of 2-mb, 3-mb, and 6-mb, respectively. They also confirmed the π -hydrogen bonded structure of these complexes from DFT calculations. The excellent agreement between solution phase FTIR and jet-cooled IR spectroscopy data on these molecular complexes is noteworthy.

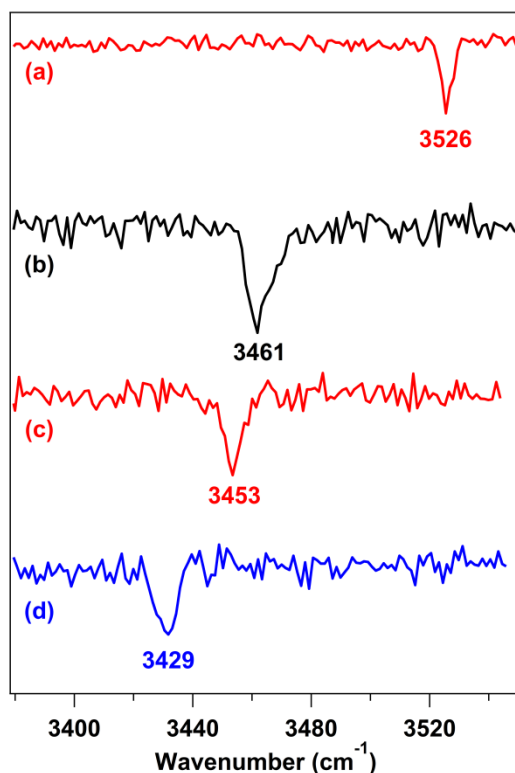


Figure 3: RIDIR spectra by probing (a) 0_0^0 band of indole, and band maxima of the broad R2PI spectra of (b) indole-2-methylbenzene dimer, (c) indole-3-methylbenzene dimer and (d) indole-6-methylbenzene dimer in the N-H stretching vibrational region.

The trend in the observed red-shift in the N-H stretching frequency in the indole-methylated benzenes compared to that in the indole-benzene complexes is quite logical as the strength of the π -hydrogen bonding acceptor increases with the increase of the electron donating groups in the benzene ring. A similar trend in the red-shift in the N-H stretching frequency has been reported for the complexes of pyrrole with benzene, pyrrole, 1-methyl pyrrole and 1,2,5-trimethyl pyrrole using either jet-FTIR or jet-IR-UV double resonance spectroscopy.^[15, 21]

Increase in the red-shift in the N-H stretching frequency with the increase of the strength of the π -hydrogen bond acceptor has also been observed for the complexes of indole with furan and thiophene.^[16-17] However, as mentioned earlier, the aim of the present work is to explore subtle changes in the structure as well as electrostatic, dispersion and steric interactions with systematic increase of the methyl substitution in the hydrogen bond acceptor moiety of the π -hydrogen bonded complexes. The following theoretical section is focused on addressing this objective in light of the observed experimental results.

C. Theoretical results

To place the experimental results obtained on the complexes of the methylated benzenes with indole into context, the structures and the properties of the indole-benzene (ind-ben) complex have been investigated using theoretical calculations. Recently, Biswal *et al.* reported four conformers of ind-ben, namely parallel displaced (PD), T-shaped (T), tilted parallel displaced (tilted PD) and tilted T-shaped (tilted T) using a variety of quantum chemical theories (DF-MP2, B97-D, PBE1-DCP) although only the tilted T structure was observed in their gas phase experiment.^[23] It is worth mentioning that they did not find all four conformers at a single level of theory. In the present study the structures of these four conformers have been optimized at the SCSN level of theory. A normal mode analysis reveals that the T structure is a transition state between two symmetrical tilted T conformers. To avoid any confusion between the tilted T and tilted PD nomenclature herein these two structures are referred to as tilted structure 1 (Tilted S1) and tilted structure 2 (Tilted S2), respectively, with respect to the definition provided in the Figure 1. The structures of the three stable conformers of the ind-ben complex optimized at the SCSN level of theory are shown in Figure 4, while the optimized SCSN parameters (R and θ) for all the four conformers are presented in Table 1. In the following the energy of the interaction between subunits is presented as both binding energy and interaction energy. The former denotes the difference in energy between the optimized geometry of the complex and the energies of the two subunits in their isolated geometries, with ZPE corrections applied. Meanwhile, the interaction energy freezes the subunits in their interacting geometry, without ZPE correction. The interaction energy is necessary for comparison with results from symmetry adapted perturbation theory (SAPT).

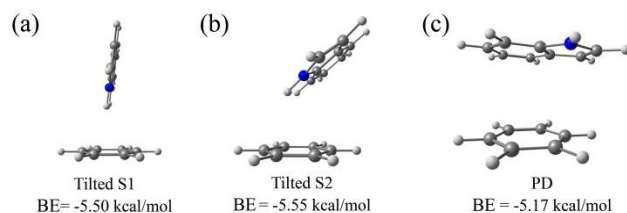


Figure 4. Optimized structures of three stable conformers of indole-benzene dimer calculated at the SCSN/aVTZ* level of theory. BE is the binding energy. The T-shaped structure has been found to be a transition state.

To facilitate comparison with experiment, the SCSN harmonic vibrational frequencies of the N–H stretch have been scaled by a constant factor of 0.92726, which was obtained by comparing the SCSN frequency of this mode in isolated indole with the experimental value of 3526 cm^{-1} . These scaled frequencies are presented alongside the SCSN binding energies in Table I. Single point CCSD(T*)-F12a binding energies are also computed for the SCSN structures, with the SCSN ZPE correction applied to produce a binding energy. From Table I it can be seen that the PD structure is less strongly bound than the other conformers by roughly 0.5 kcal/mol. The N–H stretching frequency of PD is also shifted relative to the other conformers and the experimental value. The N–H frequency and binding energy of the three remaining conformations (recalling that the T-shaped structure is a transition state) are very similar. This is especially apparent for the CCSD(T*)-F12a binding energies where the agreement is within 0.03 kcal/mol, and the vibrational frequencies have a range of 18 cm^{-1} . If the T-shaped structure is discounted then the agreement between the structures improves to 0.02 kcal/mol and 3 cm^{-1} , beyond reasonable estimates for the accuracy of the methods used.

Table I. Summary of the SCSN calculated distance between the ring centres (R), ring tilt angle (θ), N-H frequency, and binding energy (BE) for various conformers of the indole-benzene complex.

Conformation	R (Å)	θ (degrees)	N–H frequency (cm^{-1})	BE (kcal/mol)	
				SCSN	CCSD(T*)-F12a ^[a]
PD	3.795	6.6	3522	-5.17	-4.81
T ^b	4.447	89.2	3484	-5.49	-5.31
Tilted S1	4.223	55.7	3466	-5.50	-5.32
Tilted S2	4.042	39.3	3469	-5.55	-5.34
Experiment			3479 ^[c]		5.21 ^[d]

^aCalculated on the SCSN optimized geometry and including the SCSN ZPE correction.

^bThe T conformation is a transition state, but the data are provided for comparative purposes.

^cFDIR data from Biswal et al.^[23] ^dMATI data from Braun et al.^[14]

The agreement with experiment is also excellent, roughly 10 cm^{-1} for the N–H stretching frequency and 0.1 kcal/mol for the binding energy. This clearly indicates that both tilted S1 and tilted S2 can be assigned as the structures of the indole-benzene dimer and that a mixture of these two conformers may be observed. The previous work of Biswal *et al.* used DFT based methods to conclude an assignment of the tilted T-shaped (named here as tilted S1) structure, but the tilted PD (named here as tilted S2) structure was not located with the functionals selected in that investigation.^[23] The level of agreement between the CCSD(T*)-F12a and SCSN binding energies lends extra confidence to the present results, with SCSN overbinding by a mean average of only 0.23 kcal/mol.

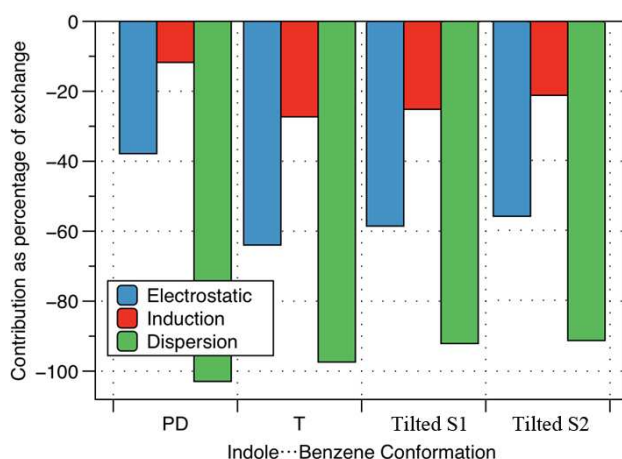


Figure 5. SAPT decomposition (SAPT2+/aug-cc-pVDZ) of the interaction energy of all the conformations of the indole-benzene dimer, presented as percentages of the exchange term.

The decomposition of the interaction energy into the chemically familiar terms of electrostatic, exchange, induction and dispersion was carried out at the SAPT2+ level. In order to analyze the resulting data, the electrostatic, induction and dispersion contributions are presented in Figure 5 as percentages of the exchange term, which eases the comparison of the data for different conformers. The individual energetic contributions of all the four terms are tabulated in the Table S1 of the supporting information. The trends in Figure 5 are somewhat as expected, the PD conformer has a reduced electrostatic contribution compared to the structures with an N-H $\cdots\pi$ interaction and is overall dominated by dispersion. PD and T-shaped conformers of indole-benzene dimer are included in the S22 database of non-covalent interactions, and previous DFT-SAPT calculations on the structures provided in that database have defined the interactions as dispersion-dominated and mixed-character, respectively, which is in good agreement with the present results.^[81] The tilted S1 and tilted S2 conformers, which represent more stable interactions than the structures in the S22 database, have a very similar SAPT decomposition that, like the T conformer, is described as a mixed-character interaction using the same criteria of Gráfová et al.^[81]

When complexes of methylated benzenes with indole are considered it is quickly apparent that there are a number of minima on each potential energy surface. In some cases idealized PD and T-shaped conformers are located, but their binding energies indicate that they are somewhat less stable than the tilted conformers with a primary N-H $\cdots\pi$ interaction. Within those tilted conformers there are two main classes of complex, separated by a difference in secondary C-H $\cdots\pi$ interactions. These interactions are between a methyl hydrogen on the substituted benzene and either the phenyl ring (Tilted S1) or the pyrrole ring (Tilted S2) of the indole sub-unit. A conformation with a C-H $\cdots\pi$ interaction between a methyl hydrogen on the substituted benzene and the pyrrole ring of the indole moiety also exists with a different tilt angle relative to tilted S2 and is named tilted S2a. The structures of the stable conformers of the complexes of indole with methylated benzenes calculated at the SCSN/aVTZ* level are presented in Figure 6

Binding energies, relevant intermolecular geometrical parameters (R and θ) and NH stretching frequencies of different conformers of the complexes of indole with methylated benzenes calculated at the SCSN/aVTZ* level of theory are listed in Table II. It can be seen from Table II that as the benzene moiety becomes increasingly methylated the magnitude of the binding energy increases and the N-H stretching frequency is red shifted, indicating a greater interaction between indole N-H and the substituted benzene. These results are in good agreement with the experimental IR spectra of the indole-methylated benzenes presented in Figure 3. A comparison of the binding energies of different conformers of the indole-methylated benzenes listed in Table II reveals that the conformers with a phenyl-methyl (Tilted S1) secondary interaction are slightly more strongly bound than those with a pyrrole-methyl (Tilted S2 or Tilted S2a) secondary interaction (by an average of 0.19 kcal/mol).

As mentioned earlier, the PD structure is not stable in the case of most complexes and its binding energy is much less compared to that of the tilted T structures. Also, the N-H stretching frequency of the PD conformer is similar to that of the indole monomer while the experimental IR spectra of all the complexes studied here are significantly red-shifted from that of the monomer. Hence, the presence of the PD conformer in the experiment can be easily excluded.

On the other hand, the difference in the binding energies of all three tilted structures is very small and their N-H stretching frequencies are also within 15-20 cm^{-1} of the experimental values. It is instructive here to recall the experimental N-H stretching frequencies of indole-2-mb, indole-3-mb, and indole-6-mb complexes, which are 3461, 3453, and 3429 cm^{-1} , respectively. It is note-worthy that the observed N-H stretching frequencies of the three complexes shown in Figure 3 are more consistent with those for the tilted S2 conformer obtained from the calculations. However the binding energies are more reliable than the calculated frequencies which are computed according to harmonic approximation. The scaling factor based on the monomer which is used to correct the harmonic frequencies of the complexes has also some error as the N-H group in the monomer is not similar to that in the complex. Moreover the binding energies are calculated at a very high level of theory and these energies have an excellent agreement with those calculated at the CCSD(T)-F12a level of theory. It is also the fact that the tilted S1 is the most stable structure in the case of all the complexes and thus the possibility of the observation of this structure in the experiment could not be excluded. Thus it could be

concluded that all three tilted structures (Tilted S1, Tilted S2 and Tilted S2a) of indole...methylated benzenes may be present in the experiment and the broadening in the R2PI spectra of these complexes is likely due to their overlapping electronic transitions as well as unresolved low frequency intermolecular vibrations. Specifically, the two tilted structures (Tilted S2 and Tilted S2a) having secondary C-H... π interaction between the methyl C-H and pyrrole ring of the indole moiety are very close in energy and N-H stretching frequencies of both the conformations are within 3-5 cm^{-1} of the experimental values. The C-H stretching frequency could not be probed through experiment as the IR intensity of the C-H transition has been found to be very weak.

Interaction energies (without relaxation of the monomers into their isolated geometries or ZPE correction) of the tilted S1 structure of indole...methylated benzenes calculated at the SCSN level are also compared with those obtained at the CCSD(T*)-F12a and other levels of calculations in Table III. It is seen that the agreement between SCSN and CCSD(T*)-F12a level values is again remarkable here. This provides additional confidence in the interpretation of the observed broad electronic spectra of indole...methylated benzenes in terms of overlapping electronic transitions of multiple conformers with closely spaced energies. The B97-D method overestimates the strength of the interaction, in some cases by greater than 1 kcal/mol, bringing into question its suitability for investigating interactions of the type observed in the present complexes. It should be noted that the interaction energy of ind...6-mb could not be calculated at the CCSD(T*)-F12a level due to prohibitively large computational cost.

Table II. Binding energies (BE), intermolecular parameters (R, θ) and scaled N-H stretching frequencies ($\nu(\text{N-H})$) of various conformers of indole...methylated benzenes calculated at the SCSN/aVTZ* level of theory

Experimental N-H stretching frequencies of ind...2-mb, ind...3-mb, and ind...6-mb are observed at [a] 3461, [b] 3453 and [c] 3429 cm^{-1} , respectively. PD structures are stable only for ind...4-mb and ind...6-mb.

Complex	Conformer	BE (kcal/mol)	$\nu(\text{N-H})$ (cm^{-1})	R (Å)	θ ($^\circ$)
ind...1-mb	Tilted S1	-7.13	3484	3.795	18.9
	Tilted S2	-7.04	3472	3.933	25.3
	Tilted S2a	-7.02	3469	3.960	27.0
ind...2-mb ^[a]	Tilted S1	-7.16	3475	3.819	22.1
	Tilted S2	-7.12	3462	3.957	28.2
ind...3-mb ^[b]	Tilted S1	-7.62	3473	3.758	20.6
	Tilted S2	-7.49	3454	3.932	29.5
	Tilted S2a	-7.41	3450	4.002	36.4
ind...4-mb	Tilted S1	-8.62	3455	3.858	26.5
	Tilted S2	-8.46	3449	3.929	31.9
	PD	-6.19	3521	4.593	6.2
ind...5-mb	Tilted S1	-9.26	3479	3.670	15.1
	Tilted S2	-9.18	3436	3.915	35.0
	Tilted S2a	-8.83	3433	4.052	46.7
ind...6-mb ^[c]	Tilted S1	-9.36	3459	3.751	21.1
	Tilted S2	-9.18	3434	3.869	30.7
	Tilted S2a	-9.04	3430	4.161	62.0
	PD	-7.28	3521	4.665	4.6

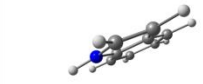
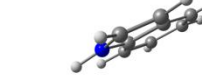
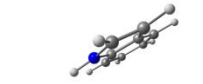
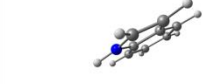
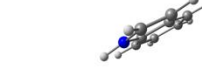
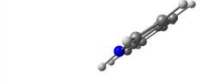
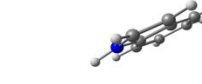
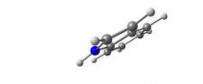
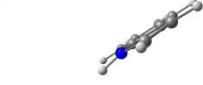
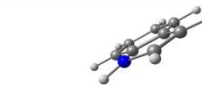
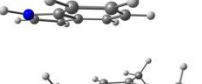
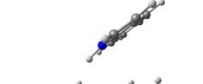

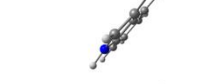
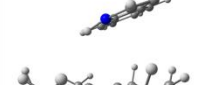
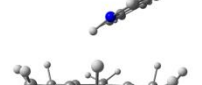

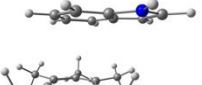
	Tilted S1	Tilted S2	Tilted S2a	PD
ind...1-mb dimer	 BE = -7.13 kcal/mol	 BE = -7.04 kcal/mol	 BE = -7.02 kcal/mol	—
ind...2-mb dimer	 BE = -7.16 kcal/mol	 BE = -7.12 kcal/mol	—	—
ind...3-mb dimer	 BE = -7.62 kcal/mol	 BE = -7.49 kcal/mol	 BE = -7.41 kcal/mol	—
ind...4-mb dimer	 BE = -8.62 kcal/mol	 BE = -8.46 kcal/mol	—	 BE = -6.19 kcal/mol
ind...5-mb dimer	 BE = -9.26 kcal/mol	 BE = -9.18 kcal/mol	 BE = -8.83 kcal/mol	—
ind...6-mb dimer	 BE = -9.36 kcal/mol	 BE = -9.18 kcal/mol	 BE = -9.04 kcal/mol	 BE = -7.28 kcal/mol

Figure 6: Optimized geometries of the most stable conformers of (a) ind...1-mb (b) ind...2-mb, (c) ind...3-mb, (d) ind...4-mb, (e) ind...5-mb and (f) ind...6-mb dimers calculated at the SCSN/aVTZ* level of theory. BE is the binding energy

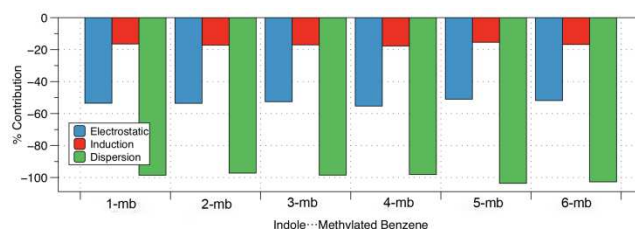
SAPT decomposition of the interaction energies of the lowest energy tilted structures (Tilted S1) of indole...methylated benzenes calculated at the SAPT2+/aVDZ level of theory is provided in Table IV. To aid in the interpretation of the SAPT decomposition, contributions of various components of the interaction energies are plotted as a percentage of the exchange term (Figure 7), where the variation between the different complexes is small. It is intriguing to note that methyl substitution in the π -hydrogen bond acceptor moiety enhances the electrostatic, dispersion and exchange-repulsion in the complexes at the same time. However, the increase in the exchange repulsion and dispersion components is slightly greater than that in the electrostatic component as the degree of methylation is increased. Using the established guidelines of Gráfová et al., the interactions can be classified as mixed-character, with the 5-mb and 6-mb complexes becoming slightly more dispersion dominated.^[81]

Table III. Comparison of interaction energies (kcal/mol) of Tilted S1 structure of indole... methylated benzenes.

System	CCSD(T*)-F12a	SCSN	SAPT	B97-D
ind...1-mb	-7.67	-7.96	-8.15	-8.15
ind...2-mb	-7.76	-8.06	-8.28	-8.30
ind...3-mb	-8.43	-8.65	-9.02	-9.08
ind...4-mb	-8.90	-9.16	-9.53	-9.66
ind...5-mb	-10.08	-10.28	-10.94	-11.13
ind...6-mb	—	-10.39	-11.02	-11.24

Table IV. SAPT decomposition of the interaction energies (kcal/mol) of the Tilted S1 structure of indole...methylated benzenes calculated at the SAPT2+/aVDZ level of theory

System	Electrostatic	Exchange	Induction	Dispersion
ind...1-mb	-6.37	11.89	-1.96	-11.72
ind...2-mb	-6.52	12.17	-2.09	-11.83
ind...3-mb	-6.96	13.25	-2.25	-13.05
ind...4-mb	-7.41	13.41	-2.38	-13.15
ind...5-mb	-7.97	15.62	-2.40	-16.18
ind...6-mb	-8.01	15.45	-2.59	-15.87

**Figure 7.** SAPT decomposition (SAPT2+/aVDZ) of the interaction energy in the Tilted T1 structure of the indole...methylated benzenes presented as percentages of the exchange term.

Conclusions

An in-depth understanding of the co-operative nature of multiple types of weak inter- and intra-molecular interactions is essential for the design and synthesis of advanced materials through self-assembly. The present work demonstrates that the structures of complexes of indole with *n*-methylated benzene (ind...*n*-mb, *n* = 1-6) are determined by a primary N-H... π interaction, along with secondary C-H... π and π ... π interactions. This corresponds to a delicate balance of steric crowding with electrostatic and dispersion forces, which has been determined through a combination of supersonic jet experiments and quantum chemical calculations.

Experimental data have been obtained for ind...*n*-mb with *n* = 2, 3, and 6 in a supersonic jet using one-color and two-color R2PI, IR-UV double resonance spectroscopic techniques, while quantum chemical calculations have been performed on all six complexes of indole with methylated benzenes. The electronic spectra of the three ind...*n*-mb (*n* = 2, 3, 6) dimers measured by $S_1 \leftarrow S_0$ excitation of the indole moiety using R2PI spectroscopy are completely broad and structureless. Comparison of the experimental IR spectra (N-H stretch region) with the computed SCSN IR spectra of various conformers of ind...*n*-mb complexes reveal that multiple tilted structures (denoted tilted S1, tilted S2 and tilted S2a) possessing similar interaction energies and N-H stretching frequencies are present in the experiment. Therefore, broadening in the electronic spectra of these complexes may be due to the overlapping electronic transitions of multiple tilted conformers as well as their unresolved low frequency intermolecular vibrations. The current work employing SCSN and CCSD(T*)-F12a calculations also highlights that at least two tilted structures could be responsible for the observed electronic spectrum of indole...benzene reported in the literature. The IR spectra also display an increase in the red-shift of

the N–H stretching frequency as the number of methyl groups is incremented. This increase in strength of the N–H $\cdots\pi$ interaction is also reflected in the benchmark structure interaction energies calculated for all six complexes.

Analysis of the optimized structures indicates that the tilted ind $\cdots n$ -mb complexes are primarily bound by an N–H $\cdots\pi$ interaction, with additional stability due to C–H $\cdots\pi$ and $\pi\cdots\pi$ secondary interactions. Computed binding energies favor the tilted S1 conformations, which possess a C–H $\cdots\pi$ interaction between a methyl hydrogen and the phenyl ring of the indole. Any parallel displaced structures located on the potential energy hypersurface are significantly less strongly bound than the tilted motifs. It is striking that the tilted S1 angle (θ) in ind $\cdots 1$ mb complexes changes greatly compared to that in ind \cdots ben but the tilt angles don't change very much for successive methylation. SAPT-based decomposition of the interaction energies highlights that the ind $\cdots n$ -mb complexes fall into the category of mixed complexes having significant contributions from both electrostatic and dispersion interactions. Overall, the present work clearly shows how subtle interplay among different components of the interaction energy in weakly bound intermolecular complexes, i.e. electrostatic, dispersion and steric repulsion, govern the specific structural motif.

Experimental Section

The experimental setup has been described in detail elsewhere and only a brief description has been provided here.^[18] The experiments were performed using a home-built jet-cooled resonantly enhanced multi-photon ionization (REMPI) time-of-flight mass spectrometer (TOFMS). The heterodimers of indole (ind) with 1,4-dimethylbenzene (2-mb), 1,3,5-trimethylbenzene (3-mb) and hexamethylbenzene (6-mb) were synthesized in a supersonic jet. Indole (99.99%, Sigma-Aldrich) was placed in a stainless steel sample holder kept behind the pulsed valve (0.5 mm diameter nozzle, General valve, series 9, rep. rate 10 Hz) and heated at 80 °C. Argon (40 psig) as a buffer gas was bubbled through 2-mb (99%, Sigma-Aldrich), 3-mb (98% Sigma-Aldrich) and 6-mb (99%, Sigma-Aldrich) maintained at -78 °C, 25 °C and 75 °C, respectively and co-expanded with indole through the nozzle.

The jet-cooled molecular beam of the complexes was ionized using one-color and two-color resonant two photon ionization (1C/2C-R2PI) spectroscopy. Frequency doubled output (about 250 μ J pulse energy) of a tunable dye laser (ND6000, Continuum) pumped by second harmonic of a Nd:YAG laser (nanosecond, 10 Hz, Surelite II-10, Continuum) was used for 1C-R2PI. For the 2C-R2PI spectroscopy, the same dye laser (about 80 μ J pulse energy) was used as the excitation laser and about 800 μ J pulse energy from another dye laser (ND6000, Continuum) was used as for the ionization. Mass-selected ions were detected in a time-of-flight mass spectrometer (Jordan TOF products). The ion signal from the detector was amplified by a preamplifier (SRS, Model SR445A) and further sent to a digital oscilloscope (Tektronix, 350 MHz, DPO 4034) interfaced with a computer. Home-built LabVIEW (National Instruments, 8.6 version) based programs were used for the data acquisition. A digital delay generator (BNC, Model 575) was used for synchronization of various lasers and the pulsed valve.

Resonant ion dip infrared spectroscopy (RIDIRS) was used to measure the IR spectra of the complexes. In this technique, counter-propagating IR laser beam (pulse energy 2–3 mJ) and UV laser beam (pulse energy 250 μ J) were spatially overlapped and intersected by the molecular beam at a right angle. The IR laser was fired 100 ns prior to the UV laser and scanned through the vibrational transitions in the ground electronic state while the UV laser was fixed to a particular transition in the R2PI spectrum of the dimer. A depletion in the R2PI ion signal occurs when the IR laser frequency matches with any vibrational transition of the dimer. Tunable IR laser radiation of typical resolution of about 2–3 cm^{-1} was obtained from a KTP/KTA based Optical Parametric Oscillator/Optical Parametric Amplifier (OPO/OPA, Laser Vision) pumped by an Unseeded Nd:YAG (ns, 10Hz, Surelite II-10) laser.

Computational Section

Geometry optimizations and the numerical calculation of harmonic vibrational frequencies were carried out in molpro^[62–83] with the density fitted SCSN local Møller-Plesset second order perturbation theory (DF-SCSN-LMP2) method, where SCSN denotes that SCS parameters were selected that have been optimized for weak and stacking interactions.^[63–64] The parallel-spin electron pair contribution to the MP2 energy is scaled by a factor of 1.76 and the antiparallel contribution is neglected. An aVTZ* basis was used, which represents the correlation consistent cc-pVTZ basis on H atoms and aug-cc-pVTZ on all other atoms.^[84–85] The DF-SCSN-LMP2/aVTZ* level of theory will be referred to as simply SCSN herein. The Hartree-Fock reference was density fitted using the cc-pVTZ/JKFit auxiliary basis set of Weigend, while density fitting at the MP2 level used the aug-cc-pVTZ/MP2Fit auxiliary sets of Weigend et al.^[86–87] The local electron correlation treatment carried out the orbital domain selection as described by Boughton and Pulay with a completeness criterion of 0.985, a minimum Mulliken charge of 0.18 was required for a hydrogen atom to be included in a domain, and all domains with two or more atoms in common were merged.^[88–90] Orbital localisation was performed using the Pipek-Mezey method and to ensure well localised orbitals the two most diffuse functions of each angular momentum type were deleted by eliminating their contribution to the localisation criterion.^[91] Both the geometry optimisation and frequency calculations were carried out with so-called floating domains, which have been demonstrated to introduce almost negligible errors relative to frozen domains.^[92] The SCSN single point calculations of the interaction energy used frozen domains determined at an intermolecular separation of 100 Å.

DFT calculations were carried out using the B97 functional, with an empirical dispersion correction (B97-D), in the Gaussian09 program package.^[93–95] These calculations used the cc-pVTZ basis for all elements and a pruned integration grid with 99 radial shells and 590 angular points per shell. The DFT interaction energies were corrected for basis set superposition error (BSSE) with the counterpoise (CP) method of Boys and Bernardi, but the geometry optimisation and Hessian calculations were not corrected.^[58] The local correlation methods are free from BSSE by construction (although the small degree of BSSE from the Hartree-Fock reference remains), meaning that SCSN does not require CP correction.^[96] Explicitly correlated coupled cluster with single, double and perturbative triple excitations [CCSD(T*)-F12a] CP-corrected single point interaction energies were calculated on the SCSN optimised geometries using the aug-cc-pVDZ basis set and the matching OptRI auxiliary basis of Yousaf and Peterson, with a geminal Slater exponent of 1.1 a_0^{-1} .^[59, 97–98] The (T*) denotes that the perturbative triples, which are not explicitly correlated, were scaled as:

$$E^{(T^*)} = E(T) \frac{E^{\text{MP2-F12}}}{E^{\text{MP2}}}$$

To ensure size-consistency, the scaling factor for the dimer was also used for each individual sub-unit.^[99] This model chemistry was recently demonstrated to produce very small mean absolute errors (0.10 kcal mol⁻¹) relative to a database of rigorous benchmark interaction energies.^[100]

SAPT calculations were carried out at the SAPT2+/aug-cc-pVDZ level on the SCSN geometries.^[101] This SAPT model chemistry was recently recommended as a “silver standard” for the calculation of non-covalent interaction energies, with a mean absolute error of 0.30 kcal mol⁻¹ when compared to a relatively large database of benchmark quality data.^[102] The gold standard of SAPT2+(3)δMP2/aug-cc-pVTZ is beyond the reach of the computational resources available to the current investigation. The SAPT calculations were carried out using density fitting and MP2 natural orbital approximations in the Psi4 (beta 5) program, and the SAPT terms have been collected into a “chemist’s grouping” that is fully detailed in the supporting information.^[103-104]

Acknowledgements

Financial support from Indian Institute of Science Education and Research (IISER), Pune to carry out this research is highly acknowledged. S.K.S. thanks IISER Pune for the senior research fellowship. Computational support from IISER Pune supercomputer facility is acknowledged by A.D. and S.K.S. The authors thank Science and Engineering Research Board (SERB), India (Grant No. EMR/2015/000486) for providing partial financial support to perform this research.

Keywords: Laser spectroscopy • Vibrational spectroscopy • Noncovalent interactions • Ab initio calculation • Electronic spectroscopy

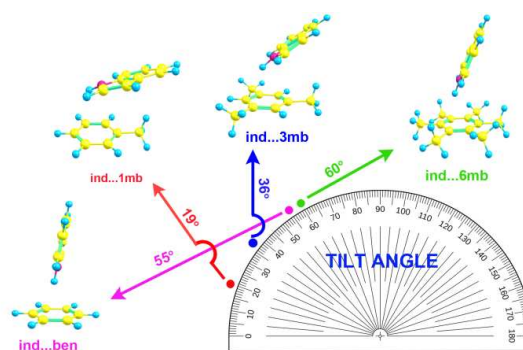
- [1] E. G. Brown, *Ring Nitrogen and Key Biomolecules*, Springer Netherlands, Dordrecht, **1998**.
- [2] S. K. Burley, G. A. Petsko, *FEBS letters* **1986**, *203*, 139.
- [3] M. Levitt, M. F. Perutz, *J. Mol. Biol.* **1988**, *201*, 751.
- [4] E. A. Meyer, R. K. Castellano, F. Diederich, *Angew. Chem. Int. Ed.* **2003**, *42*, 1210.
- [5] G. Duan, V. H. Smith, D. F. Weaver, *J. Phys. Chem. A* **2000**, *104*, 4521.
- [6] R. M. Hughes, M. L. Waters, *J. Am. Chem. Soc.* **2006**, *128*, 13586.
- [7] G. Tóth, R. F. Murphy, S. Lovas, *J. Am. Chem. Soc.* **2001**, *123*, 11782.
- [8] S. Sarkhel, G. R. Desiraju, *Proteins: Struct. Funct. Bioinf.* **2004**, *54*, 247.
- [9] G. R. Desiraju, T. Steiner, *The Weak Hydrogen Bond: In Structural Chemistry and Biology*, Oxford University Press, **2001**.
- [10] T. Steiner, *Angew. Chem. Int. Ed.* **2002**, *41*, 48.
- [11] T. Steiner, G. Koellner, *J. Mol. Biol.* **2001**, *305*, 535.
- [12] J. F. Malone, C. M. Murray, M. H. Charlton, R. Docherty, A. J. Lavery, *J. Chem. Soc. Faraday Trans.* **1997**, *93*, 3429.
- [13] G. A. Worth, R. C. Wade, *J. Phys. Chem.* **1995**, *99*, 17473.
- [14] J. Braun, H. J. Neusser, P. Hobza, *J. Phys. Chem. A* **2003**, *107*, 3918.
- [15] I. Dauster, C. A. Rice, P. Zielke, M. A. Suhm, *Phys. Chem. Chem. Phys.* **2008**, *10*, 2827.
- [16] S. Kumar, V. Pande, A. Das, *J. Phys. Chem. A* **2012**, *116*, 1368.
- [17] S. Kumar, A. Das, *J. Chem. Phys.* **2012**, *137*, 094309.
- [18] S. Kumar, P. Biswas, I. Kaul, A. Das, *J. Phys. Chem. A* **2011**, *115*, 7461.
- [19] M. Mons, I. Dimicoli, B. Tardivel, F. Piuzy, V. Brenner, P. Millié, *Phys. Chem. Chem. Phys.* **2002**, *4*, 571.
- [20] P. Ottiger, C. Pfaffen, R. Leist, S. Leutwyler, R. A. Bachorz, W. Klopper, *J. Phys. Chem. B* **2009**, *113*, 2937.
- [21] C. Pfaffen, D. Infanger, P. Ottiger, H.-M. Frey, S. Leutwyler, *Phys. Chem. Chem. Phys.* **2011**, *13*, 14110.
- [22] M. Saggiu, N. M. Levinson, S. G. Boxer, *J. Am. Chem. Soc.* **2012**, *134*, 18986.
- [23] H. S. Biswal, E. Gloaguen, M. Mons, S. Bhattacharyya, P. R. Shirhatti, S. Wategaonkar, *J. Phys. Chem. A* **2011**, *115*, 9485.
- [24] V. Chandrasekaran, L. Biennier, E. Arunan, D. Talbi, R. Georges, *J. Phys. Chem. A* **2011**, *115*, 11263.
- [25] M. Pitoňák, P. Neogrady, J. Řezáč, P. Jurečka, M. Urban, P. Hobza, *J. Chem. Theory Comput.* **2008**, *4*, 1829.
- [26] W. Wang, M. Pitoňák, P. Hobza, *ChemPhysChem* **2007**, *8*, 2107.
- [27] K. O. Börnsen, H. L. Selzle, E. W. Schlag, *J. Chem. Phys.* **1986**, *85*, 1726.
- [28] K. C. Janda, J. C. Hemminger, J. S. Winn, S. E. Novick, S. J. Harris, W. Klemperer, *J. Chem. Phys.* **1975**, *63*, 1419.
- [29] J. Řezáč, P. Hobza, *J. Chem. Theory Comput.* **2008**, *4*, 1835.
- [30] M. O. Sinnokrot, C. D. Sherrill, *J. Phys. Chem. A* **2004**, *108*, 10200.
- [31] S. Tsuzuki, T. Uchimaru, K.-i. Sugawara, M. Mikami, *J. Chem. Phys.* **2002**, *117*, 11216.
- [32] J. B. O. Mitchell, C. L. Nandi, I. K. McDonald, J. M. Thornton, S. L. Price, *J. Mol. Biol.* **1994**, *239*, 315.
- [33] Y. Geng, T. Takatani, E. G. Hohenstein, C. D. Sherrill, *J. Phys. Chem. A* **2010**, *114*, 3576.
- [34] D. A. Rodham, S. Suzuki, R. D. Suenram, F. J. Lovas, S. Dasgupta, W. A. Goddard, G. A. Blake, *Nature* **1993**, *362*, 735.
- [35] G. R. Desiraju, *J. Chem. Sci. (Bangalore, India)* **2010**, *122*, 667.
- [36] E. C. Lee, D. Kim, P. Jurečka, P. Tarakeshwar, P. Hobza, K. S. Kim, *J. Phys. Chem. A* **2007**, *111*, 3446.
- [37] E. Arunan, H. S. Gutowsky, *J. Chem. Phys.* **1993**, *98*, 4294.
- [38] S. Ahnen, A.-S. Hehn, K. D. Vogiatzis, M. A. Trachsel, S. Leutwyler, W. Klopper, *Chem. Phys.* **2014**, *441*, 17.
- [39] C. E. Dessent, W. D. Geppert, S. Ullrich, K. Müller-Dethlefs, *Chem. Phys. Lett.* **2000**, *319*, 375.
- [40] D. Reha, H. Valdes, J. Vondrasek, P. Hobza, A. Abu-Riziq, B. Crews, M. S. de Vries, *Chem.-Eur. J.* **2005**, *11*, 6803.
- [41] J. Rezac, D. Nachtigallova, F. Mazzoni, M. Pasquini, G. Pietraperzia, M. Becucci, K. Muller-Dethlefs, P. Hobza, *Chem.-Eur. J.* **2015**, *21*, 6740.
- [42] E. G. Buchanan, W. H. James, 3rd, S. H. Choi, L. Guo, S. H. Gellman, C. W. Muller, T. S. Zwier, *J. Chem. Phys.* **2012**, *137*, 094301.

- [43] Z. Gengeliczki, M. P. Callahan, M. Kabelac, A. M. Rijs, M. S. de Vries, *J. Phys. Chem. A* **2011**, *115*, 11423.
- [44] S. Jaque, W. Du, E. J. Meijer, J. Oomens, A. M. Rijs, *J. Phys. Chem. A* **2013**, *117*, 1216.
- [45] E. Aguado, I. Leon, J. Millan, E. J. Cocinero, S. Jaque, A. M. Rijs, A. Lesarri, J. A. Fernandez, *J. Phys. Chem. B* **2013**, *117*, 13472.
- [46] B. C. Dian, A. Longarte, S. Mercier, D. A. Evans, D. J. Wales, T. S. Zwier, *J. Chem. Phys.* **2002**, *117*, 10688.
- [47] A. G. Abo-Riziq, B. Crews, J. E. Bushnell, M. P. Callahan, M. S. De Vries, *Mol. Phys.* **2005**, *103*, 1491.
- [48] R. A. Bachorz, F. A. Bischoff, S. Hofener, W. Klopper, P. Ottiger, R. Leist, J. A. Frey, S. Leutwyler, *Phys. Chem. Chem. Phys.* **2008**, *10*, 2758.
- [49] I. Leon, J. Millan, E. J. Cocinero, A. Lesarri, F. Castano, J. A. Fernandez, *Phys. Chem. Chem. Phys.* **2012**, *14*, 8956.
- [50] H. Fricke, A. Gerlach, C. Unterberg, P. Rzepecki, T. Schrader, M. Gerhards, *Phys. Chem. Chem. Phys.* **2004**, *6*, 4636.
- [51] C. Pfaffen, H.-M. Frey, P. Ottiger, S. Leutwyler, R. A. Bachorz, W. Klopper, *Phys. Chem. Chem. Phys.* **2010**, *12*, 8208.
- [52] R. N. Pribble, T. S. Zwier, *Science* **1994**, *265*, 75.
- [53] M. Saggiu, N. M. Levinson, S. G. Boxer, *J. Am. Chem. Soc.* **2011**, *133*, 17414.
- [54] M. A. Trachsel, P. Ottiger, H.-M. Frey, C. Pfaffen, A. Bihlmeier, W. Klopper, S. Leutwyler, *J. Phys. Chem. B* **2015**, *119*, 7778.
- [55] J. A. Frey, C. Holzer, W. Klopper, S. Leutwyler, *Chem. Rev.* **2016**, *116*, 5614.
- [56] F. Biedermann, H.-J. Schneider, *Chem. Rev.* **2016**, *116*, 5216.
- [57] J. Řezáč, P. Hobza, *Chem. Rev.* **2016**, *116*, 5038.
- [58] S. F. Boys, F. Bernardi, *Mol. Phys.* **1970**, *19*, 553.
- [59] G. Knizia, T. B. Adler, H.-J. Werner, *J. Chem. Phys.* **2009**, *130*, 054104.
- [60] C. Hättig, W. Klopper, A. Köhn, D. P. Tew, *Chem. Rev.* **2012**, *112*, 4.
- [61] D. A. Sirianni, L. A. Burns, C. D. Sherrill, *J. Chem. Theory Comput.* **2016**.
- [62] T. Korona, D. Kats, M. Schütz, T. B. Adler, Y. Liu, H.-J. Werner, in *Linear-Scaling Techniques in Computational Chemistry and Physics: Methods and Applications* (Eds.: R. Zalesny, M. G. Papadopoulos, P. G. Mezey, J. Leszczynski), Springer Netherlands, Dordrecht, **2011**, pp. 345.
- [63] S. Grimme, *J. Chem. Phys.* **2003**, *118*, 9095.
- [64] J. G. Hill, J. A. Platts, *J. Chem. Theory Comput.* **2007**, *3*, 80.
- [65] J. G. Hill, J. A. Platts, *Phys. Chem. Chem. Phys.* **2008**, *10*, 2785.
- [66] J. G. Hill, J. A. Platts, *Chem. Phys. Lett.* **2009**, *479*, 279.
- [67] X. Lu, H. Shi, J. Chen, D. Ji, *Comp. Theor. Chem.* **2012**, *982*, 34.
- [68] J.-I. Seo, I. Kim, Y. S. Lee, *Chem. Phys. Lett.* **2009**, *474*, 101.
- [69] M. O. Sinnokrot, C. D. Sherrill, *J. Phys. Chem. A* **2006**, *110*, 10656.
- [70] M. O. Sinnokrot, E. F. Valeev, C. D. Sherrill, *J. Am. Chem. Soc.* **2002**, *124*, 10887.
- [71] S. Tsuzuki, T. Uchimaru, M. Mikami, K. Tanabe, *Chem. Phys. Lett.* **1996**, *252*, 206.
- [72] J. G. Hill, J. A. Platts, H.-J. Werner, *Phys. Chem. Chem. Phys.* **2006**, *8*, 4072.
- [73] G. Columberg, A. Bauder, *J. Chem. Phys.* **1997**, *106*, 504.
- [74] Y. Matsumoto, K. Honma, *Phys. Chem. Chem. Phys.* **2011**, *13*, 13962.
- [75] J. W. Hager, D. R. Demmer, S. C. Wallace, *J. Phys. Chem.* **1987**, *91*, 1375.
- [76] J. Hager, S. C. Wallace, *J. Phys. Chem.* **1984**, *88*, 5513.
- [77] L. Muzangwa, S. Nyambo, B. Uhler, S. A. Reid, *J. Chem. Phys.* **2012**, *137*, 184307.
- [78] S. A. Reid, S. Nyambo, L. Muzangwa, B. Uhler, *J. Phys. Chem. A* **2013**, *117*, 13556.
- [79] W. Lu, Y. Hu, Z. Lin, S. Yang, *J. Chem. Phys.* **1996**, *104*, 8843.
- [80] J. R. Carney, T. S. Zwier, *J. Phys. Chem. A* **1999**, *103*, 9943.
- [81] L. Gráfová, M. Pitoňák, J. Řezáč, P. Hobza, *J. Chem. Theory Comput.* **2010**, *6*, 2365.
- [82] MOLPRO, a package of ab initio programs, H.-J. Werner, P. J. Knowles, G. Knizia, F. R. Manby, M. Schütz, et al. see <http://www.molpro.net>.
- [83] H.-J. Werner, P. J. Knowles, G. Knizia, F. R. Manby, M. Schütz, *Wiley Interdiscip. Rev. Comput. Mol. Sci.* **2012**, *2*, 242.
- [84] T. H. Dunning, *J. Chem. Phys.* **1989**, *90*, 1007.
- [85] R. A. Kendall, T. H. Dunning, R. J. Harrison, *J. Chem. Phys.* **1992**, *96*, 6796.
- [86] F. Weigend, *Phys. Chem. Chem. Phys.* **2002**, *4*, 4285.
- [87] F. Weigend, A. Köhn, C. Hättig, *J. Chem. Phys.* **2002**, *116*, 3175.
- [88] P. Pulay, *Chem. Phys. Lett.* **1983**, *100*, 151.
- [89] C. Hampel, H. J. Werner, *J. Chem. Phys.* **1996**, *104*, 6286.
- [90] J. W. Boughton, P. Pulay, *J. Comput. Chem.* **1993**, *14*, 736.
- [91] J. Pipek, P. G. Mezey, *J. Chem. Phys.* **1989**, *90*, 4916.
- [92] J. A. Platts, J. G. Hill, *Mol. Phys.* **2010**, *108*, 1497.
- [93] S. Grimme, *J. Comput. Chem.* **2006**, *27*, 1787.
- [94] M. J. Frisch, et al., GAUSSIAN 09, Revision D.01, Gaussian, Inc., Wallingford CT, 2009
- [95] A. D. Becke, *J. Chem. Phys.* **1997**, *107*, 8554.
- [96] M. Schütz, G. Rauhut, H.-J. Werner, *J. Phys. Chem. A* **1998**, *102*, 5997.
- [97] K. E. Yousaf, K. A. Peterson, *Chem. Phys. Lett.* **2009**, *476*, 303.
- [98] J. G. Hill, K. A. Peterson, G. Knizia, H.-J. Werner, *J. Chem. Phys.* **2009**, *131*, 194105.
- [99] O. Marchetti, H.-J. Werner, *J. Phys. Chem. A* **2009**, *113*, 11580.
- [100] L. A. Burns, M. S. Marshall, C. D. Sherrill, *J. Chem. Phys.* **2014**, *141*, 234111.
- [101] B. Jeziorski, R. Moszynski, K. Szalewicz, *Chem. Rev.* **1994**, *94*, 1887.
- [102] T. M. Parker, L. A. Burns, R. M. Parrish, A. G. Ryno, C. D. Sherrill, *J. Chem. Phys.* **2014**, *140*, 094106.
- [103] J. M. Turney, A. C. Simmonett, R. M. Parrish, E. G. Hohenstein, F. A. Evangelista, J. T. Fermann, B. J. Mintz, L. A. Burns, J. J. Wilke, M. L. Abrams, N. J. Russ, M. L. Leininger, C. L. Janssen, E. T. Seidl, W. D. Allen, H. F. Schaefer, R. A. King, E. F. Valeev, C. D. Sherrill, T. D. Crawford, *Wiley Interdiscip. Rev. Comput. Mol. Sci.* **2012**, *2*, 556.
- [104] E. G. Hohenstein, C. D. Sherrill, *J. Chem. Phys.* **2010**, *133*, 014101.

Table of Contents

FULL PAPER

Tilt or not to tilt: The tilt angles in π -hydrogen bonded complexes of indole...methyl substituted benzenes are governed by subtle interplay among electrostatic, dispersion and steric repulsion.



Sumit Kumar, Santosh K. Singh,
Jamuna K. Vaishnav, J. Grant
Hill* and Alope Das*

Page No. – Page No.

Title: Interplay among electrostatic, dispersion and steric interactions: Spectroscopy and quantum chemical calculations of π -hydrogen bonded complexes